

Post-irradiation cracking of H₂ and formation of interface states in irradiated metal-oxide-semiconductor field-effect transistors

R. E. Stahlbush

Naval Research Laboratory, Washington, DC 20375

<http://dx.doi.org/10.1063/1.353348>

A. H. Edwards

Department of Electrical Engineering, University of North Carolina, Charlotte, North Carolina 28223

D. L. Griscom and B. J. Mrstik

Naval Research Laboratory, Washington, DC 20375

(Received 3 October 1991; accepted for publication 28 September 1992)

Molecular hydrogen is alternately introduced into and removed from the gate oxide of irradiated metal-oxide-semiconductor field-effect transistors at room temperature by changing the ambient between forming gas (10/90% H₂/N₂) and nitrogen. Using charge pumping, it is observed that H₂ causes a simultaneous buildup of interface states and decrease of trapped positive charge. The results are explained by a reaction sequence in which H₂ is cracked to form mobile H⁺, which under positive bias drifts to the Si/SiO₂ interface, and reacts to produce a dangling-bond defect. The rate limiting step over most of the time domain studied is the cracking process. Two types of cracking sites are modeled by molecular orbital calculations: oxygen vacancies (*E'* centers) and broken bond hole traps (BBHTs). Initial- and final-state energies, as well as the activation energies, are calculated. The calculations indicate that the latter is the more likely H₂ cracking site. The combined experimental and theoretical results suggest that at least 15% of the trapped positive charge is at sites similar to the BBHT sites. Implications of the model and similarities between interface-state formation by cracked H₂ and irradiation are discussed.

I. INTRODUCTION

Hydrogen has dramatic and complex effects on metal-oxide-semiconductor (MOS) devices. For over 20 years, low-temperature (~400 °C) postmetallization anneals in forming gas have been used to reduce interface-state densities by 1–2 orders of magnitude.¹ On the other hand, experiments also show that hydrogen can have deleterious effects. It can amplify hot-electron effects^{1–3} as well as radiation effects.^{4–6} There is also evidence of hydrogen's role in interface-state formation during irradiation, provided by pulsed irradiation experiments.^{7,8} All of these experimental data were obtained for hydrogen introduced during the fabrication of the MOS device. Recent experiments have examined the effects of introducing hydrogen after fabrication. Studies of hydrogen annealing show the profound effect of temperature; depending upon the annealing temperature, interface-state densities can be raised or lowered by two orders of magnitude.⁹ Also, hydrogen introduced into previously irradiated devices increases the interface-state density severalfold.^{10,11}

The examples cited above are an indication of the intensity with which hydrogen effects have been studied. It is surprising, then, that very little is understood about the interaction mechanisms. In fact, there is very little data that exhibits direct observation of hydrogenic species in the oxide. Here is a brief summary of the direct evidence for hydrogenic species in *α*-SiO₂. In 1982 Brower, Lenahan, and Dressendorfer observed isolated hydrogen atoms through their hyperfine interactions in an electron-spin-resonance (ESR) experiment performed on MOS samples that were irradiated at 77 K.¹² The H⁰ hyperfine signal decreased rapidly above 120 K. Griscom, Stapelbroek, and Friebele made similar measurements on bulk *α*-SiO₂ and

obtained similar kinetics.^{13,14} A few years ago, Gale *et al.*¹⁵ gave the first direct evidence of hydrogen motion during avalanche injection. Using secondary-ion-mass spectroscopy (SIMS), they showed that enormous quantities of hydrogen (~10²⁰ cm⁻³) piled up at the Si/SiO₂ interface. Finally, Shelby has observed the reaction of hydrogen with irradiated hydroxyl-free, bulk *α*-SiO₂ using infrared (IR) spectroscopy.^{16,17}

We have been performing hydrogen annealing studies on previously irradiated MOS devices. In this article we report the results of a set of experiments in which molecular hydrogen is alternately introduced into and removed from a gate oxide at room temperature. We establish an unambiguous correlation between the presence of molecular hydrogen and the simultaneous growth of interface states and decay of oxide trapped positive charge. To explain this striking correlation, we elaborate on an earlier model in which we proposed that molecular hydrogen is cracked at a radiation-induced positively charged defect.¹¹ This reaction produces one bound hydrogen ion and a mobile H⁺ species. Previously, Griscom *et al.* have discussed H₂ cracking by a nonbridging oxygen atom.^{13,14} The positively charged oxygen vacancy (*E'* center)^{18,19} is another cracking site to consider. To explore the possibilities, we have performed molecular orbital calculations of two types of cracking sites: *E'* centers and broken Si—O bonds with a trapped hole (which we label BBHT). Using relatively large clusters of atoms, we have modeled the reaction and calculated activation energies for H₂ cracking. We find that the BBHT is the more likely candidate, because the cracking reaction is exothermic and the calculated activation energy is consistent with the observed reaction kinetics. Once H₂ is cracked and H⁺ is formed, we are guided by a

model for H^+ motion developed by McLean⁷ and extensively studied by Saks and Brown⁸ that successfully explains the buildup of interface states following pulsed irradiation and by interface reactions with H^+ proposed by Griscom, Brown, and Saks.²⁰ The H^+ formed by cracking moves toward the Si/SiO₂ interface under the influence of a positive gate bias. Upon reaching the interface, it captures an electron from the silicon and reacts with an interfacial Si—H bond to form H_2 and a dangling silicon orbital.

The balance of the paper is organized as follows. Sections II and III are devoted to the experimental method and results. In Sec. IV, we discuss the general aspects of the hydrogen cracking model that is central to our interpretation of the experimental results. The cracking site calculations are presented in Sec. V. We discuss the combined experimental and theoretical results and conclude in Sec. VI.

II. EXPERIMENTAL DETAILS

The MOS field-effect transistors (MOSFETs) used in this study are N channel and have polysilicon gates. The channel width is 150 μm and measurements were made on devices with lengths of 5, 10, and 15 μm . All devices exhibited the same behavior. Results from 5 and 10 μm MOSFETs are shown in this article. A dry gate oxide was grown at 1000 °C to a thickness of 770 Å. There was no capping layer following metalization so that the gate oxide was exposed to the ambient at the channel edges. Molecular hydrogen in the ambient entered at the channel edges and because hydrogen diffuses rapidly through SiO₂, the H_2 quickly permeated the gate oxide. For example, using H_2 diffusion constants from bulk SiO₂, the time for the hydrogen concentration to reach half of its equilibrium value in a 5- μm -long MOSFET at room temperature is ~ 0.2 h.^{21,22} Thus, it is possible to control the hydrogen concentration in the oxide by changing the ambient.

The transistors were x-ray irradiated in air with a tungsten tube operated at 60 kV at a dose rate of 1.8 krad(SiO₂)/s. Total doses were either 1 or 10 Mrad(SiO₂). A variety of oxide fields ranging from -1.5 to 1 MV/cm were used during irradiation. A bias of 1 MV/cm was used for the data reported here. The same postirradiation hydrogen ambient effects are observed for all irradiation conditions. Within 1 h after irradiation, the MOSFETs were mounted into a vacuum chamber and placed under bias. The chamber was evacuated or filled with an atmosphere of N_2 for several days before introducing forming gas (10/90% H_2/N_2).

The trapped positive charge N_{ot} , the number of interface states N_{it} , and the energy distribution of interface states D_{it} were monitored by charge pumping. Charge pumping was performed with the MOSFETs in the vacuum chamber. The measurement time for N_{ot} , N_{it} , and D_{it} is under 15 min making it possible to continuously monitor changes that occur with a time scale of hours or longer. The detailed method of determining these quantities has been previously described.^{11,23,24} In our measurements, interface states between about 0.2 and 0.9 eV above valence

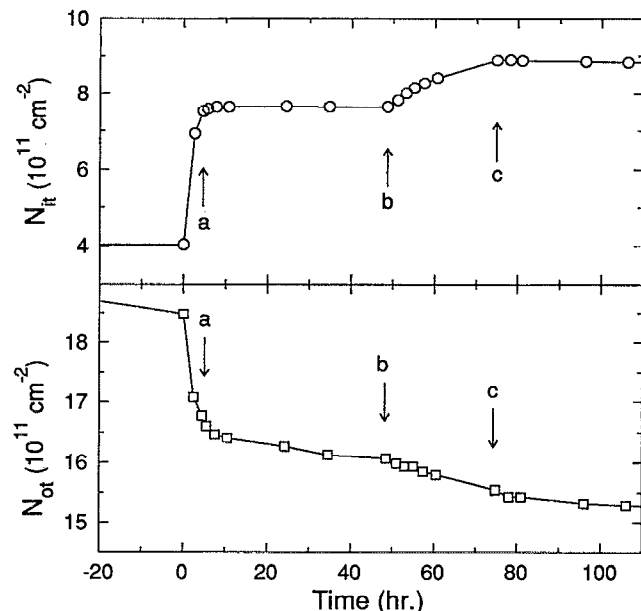


FIG. 1. The effect of the ambient upon the number of interface states N_{it} and upon the number of trapped positive charges N_{ot} in a 5- μm -long irradiated MOSFET with its gate at +5 V. Hydrogen (10/90% H_2/N_2) is introduced at 0 and 48 h and nitrogen is introduced at 4 and 76 h. Arrows a, b, and c point to the ambient changes at 4, 48, and 76 h, respectively. The MOSFET is irradiated to 1 Mrad(SiO₂) 65 h before hydrogen is first introduced.

band were measured. N_{ot} is calculated from the midgap voltage by assuming all the positive trapped charge is at the Si/SiO₂ interface. Previous work has shown that for our irradiation conditions most of the trapped charge resides within roughly 100 Å of the interface.²⁵ Furthermore, after a few days, the charges nearest the interface are neutralized by electrons tunneling from the silicon. Because the centroid of charge is not exactly at the interface, the trapped charge density is underestimated by about 10%.

III. EXPERIMENTAL RESULTS

The effect of introducing hydrogen into an irradiated gate oxide is demonstrated by alternately introducing and withdrawing the hydrogen as shown in Fig. 1. No changes are observed for unirradiated devices placed in a hydrogen ambient. The data in Fig. 1 are from a MOSFET with dimensions $W/L = 150/5 \mu\text{m}$ irradiated to 1 Mrad(SiO₂) 65 h before adding the hydrogen ambient (10/90% H_2/N_2) at $t = 0$. The bias is held at 5 V except during the 15 min intervals during which the charge pumping measurements are made. During the interval between irradiation and hydrogen introduction, N_{it} and N_{ot} change as expected. The N_{ot} decrease is proportion to $\log(t)$.²⁵ The N_{it} increases 10%–20% during the first several hours,²⁶ and subsequent changes to N_{it} before introducing the hydrogen are 2%–3%. Four ambient changes occur over the time interval of Fig. 1. Hydrogen is introduced at 0 h and at 48 h (point b in Fig. 1), and the ambient is changed back to nitrogen at 4 h (point a) and 76 h (point c). The effect of the ambient is most clearly exhibited by N_{it} . During the

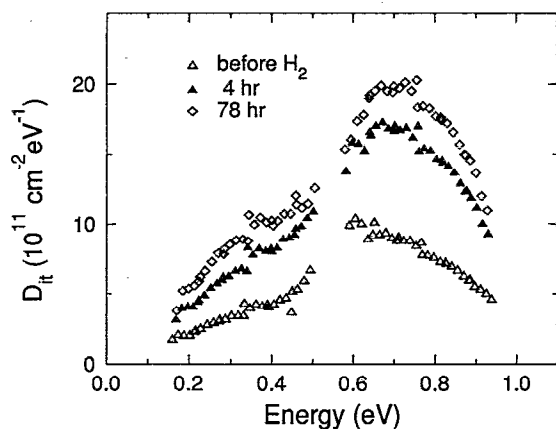


FIG. 2. The energy distribution of interface states D_{it} , before and after placing a 5- μm -long irradiated MOSFET into hydrogen (10/90% H_2/N_2). D_{it} after 4 and 76 h correspond to times a and c in Fig. 1.

first 4 h in H_2 , N_{it} doubles. In the following 44 h in N_2 , N_{it} increases a only few percent and this increase occurs in the first few hours after the ambient is changed to N_2 while H_2 is diffusing out of the gate oxide. After reintroducing H_2 at 48 h, N_{it} continues to increase until the hydrogen ambient is removed at 76 h. After a subsequent hydrogen exposure for 150 h (not shown), N_{it} stabilizes at $1.0 \times 10^{12}/\text{cm}^2$. The pattern of the N_{ot} decrease is similar although it is complicated by the annealing that is present without H_2 .²⁵ Each time hydrogen is introduced, the N_{ot} decrease is accelerated.

The energy distribution of interface states D_{it} is shown in Fig. 2 before and during the H_2 -induced buildup. The open triangles show D_{it} before the H_2 ambient and the closed triangles and open diamonds show the density at times a and c in Fig. 1, respectively. The distribution of interface states that we observe is typical of radiation-induced interface states.^{6,27} The number of states is larger in the upper half of the silicon band gap and peaks about 0.1 eV above midgap. Assuming that there are not large contributions from band-tail states outside of measurement range, we estimate that all but 10%–20% of the states are counted. For the devices measured here as well as commercial devices from a number of vendors we have examined, charge pumping does not show a turn up near the band edges after irradiation for MOSFETs with gate lengths of 10 μm or less.²⁸ For longer devices, minority-carrier recombination can produce an apparent turn up near the band edge that is an artifact. The shape of the energy distribution in Fig. 2 is also similar to the shape obtained from ESR measurements of P_b centers on (100) surfaces suggesting that we are measuring primarily P_b centers.²⁹ The shape of the distribution after H_2 exposure is the same as the shape produced by irradiation. For example, MOSFETs irradiated to 10 Mrad(SiO_2) but not exposed to hydrogen have a D_{it} curve that is similar in shape and magnitude to the D_{it} curve at time c in Fig. 1.

The data in Fig. 1 are replotted in Fig. 3 to show the roughly two-to-one ratio between the N_{it} increase and the

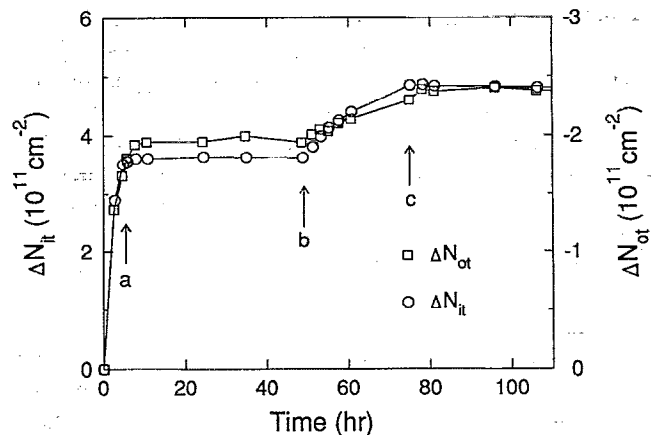


FIG. 3. Changes to the number of interface states ΔN_{it} and to the number of trapped charges ΔN_{ot} due to H_2 . The data in Fig. 1 is replotted to show the 2:1 ratio between ΔN_{it} and ΔN_{ot} . The annealing of trapped charge that occurs without hydrogen has been subtracted from the ΔN_{ot} data in this figure. Arrows a, b, and c point to the ambient changes at 4, 48, and 76 h, respectively.

N_{ot} decrease. Open circles are used for ΔN_{it} and open squares for ΔN_{ot} . The scale for ΔN_{ot} is twice the scale for ΔN_{it} and the ΔN_{ot} scale is negative. In Fig. 3, the ΔN_{ot} data are adjusted by removing the $\log(t)$ dependence that occurs without the hydrogen ambient. The rate of trapped charge decrease is $2 \times 10^{11} \text{ cm}^{-2}$ per time decade prior to the initial hydrogen ambient and this decrease is removed from the data. Given the experimental uncertainties, we expect that the ratio is accurate to within 30%. During the 150 h hydrogen anneal following this data, ΔN_{it} and ΔN_{ot} stabilize near $6 \times 10^{11}/\text{cm}^2$ and $-3 \times 10^{11}/\text{cm}^2$, respectively. These changes correspond to a 150% increase in N_{it} and a 15% decrease in N_{ot} induced by H_2 .

The polarity dependence of the H_2 induced reactions is shown in Figs. 4 and 5. The data are from MOSFETs with channel dimensions W/L of 150/10 μm that were irradiated to 10 Mrad(SiO_2). Gate biases of either -20 or 5 V were applied during the hydrogen exposure and for 20 h prior to the exposure. These voltages were chosen to be well to either side of the midgap voltage. (The midgap voltage ranged from -11 to -8 V during the hydrogen exposure.) This guarantees that the electric field is in the same direction throughout the thickness of the gate oxide. The increase of interface states ΔN_{it} and the decrease of trapped charge ΔN_{ot} are shown in Figs. 4 and 5, respectively. The ΔN_{it} data exhibit a strong polarity dependence whereas ΔN_{ot} has a weak polarity dependence. When the electric field points toward the Si/ SiO_2 interface, the buildup of interface states is four times greater than when the field points away from the interface. Note also that once the polarity has been held negative with H_2 present, changing to a positive polarity has little effect. After 95 h at -20 V , the bias was changed to $+4 \text{ V}$ for 80 h. The small increase after the positive bias is shown by the open diamond.

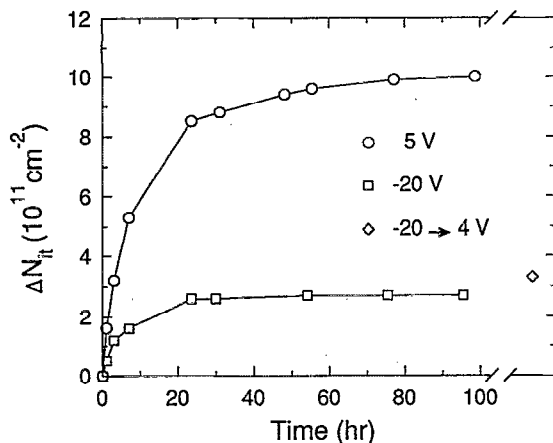


FIG. 4. Bias dependence of the interface-state buildup due to forming gas. The change in the number of interface states ΔN_{it} is shown for irradiated (10 Mrad) 10- μ m-long MOSFETs. During H_2 exposure the gate biases are 5 or -20 V. The gate bias of the MOSFET initially at -20 V is changed to 4 V at 95 h. The open diamond shows ΔN_{it} after an additional 80 h at 4 V.

IV. HYDROGEN REACTIONS

These results demonstrate the interplay between molecular hydrogen, the post-irradiation buildup of interface states, and radiation-induced trapped charge. At this point we propose a microscopic model based in part on these experiments, in part on other experiments that are explained by H^+ motion, in part on previous ESR experiments that have identified some of the important positive charge traps in α - SiO_2 produced by irradiation, and in part on theoretical calculations presented in Sec. V.

Our model for the creation of interface states is as follows. H_2 diffuses into the gate oxide of an irradiated MOS device and is cracked at a positively charged, radiation-induced defect to form H^+ . Depending on the polarity, the H^+ drifts either to the Si/ SiO_2 interface where it produces the defects responsible for interface states or to

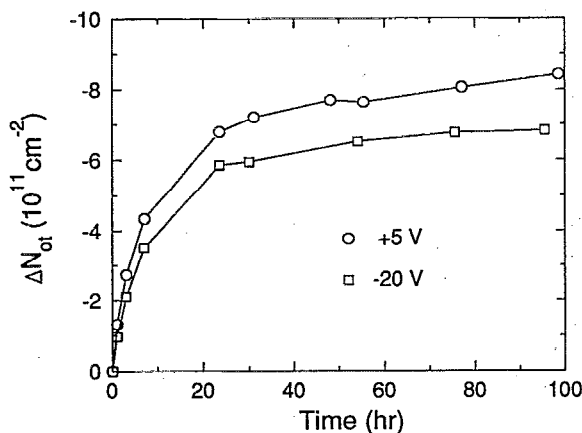
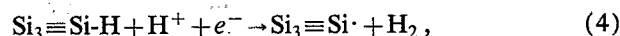
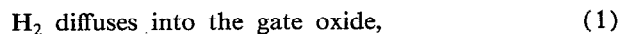


FIG. 5. Bias dependence of the trapped charge decrease due to forming gas. The change in the number of trapped charges ΔN_{ot} is shown for the same MOSFETs as in Fig. 4 with gate biases of 5 and -20 V.

the gate where its effects are not electrically observable. With positive polarity the reaction sequence is



where CS in step (2) indicates a cracking site for H_2 . Note that the cracking site on the left-hand side (lhs) of Eq. (2) is positively charged and contributes to the observed N_{ot} . Before the gate oxide is irradiated, the cracking site is not present. Equation (1) and (2) are unaffected by the polarity, but with negative polarity, H^+ in Eq. (3) drifts to the gate and Eq. (4) does not occur at the interface. After a H_2 molecule is cracked [Eq. (2)], the positive charge at the cracking site is carried away as a hydrogen ion H^+ . We defer discussion of the structure of the cracking site and of H^+ motion to the following section. Reaction sequences involving Eqs. (3) and (4) have been postulated previously to explain the results of pulsed irradiation experiments.^{7,8} Equation (4) has been suggested to explain the buildup of interface states due to irradiation.²⁰ Once H^+ reaches the Si/ SiO_2 interface, an electron from the silicon substrate tunnels into the oxide and converts the H^+ to H^0 . The H^0 reacts with Si-H to form H_2 and a P_b center [right-hand side (rhs) of Eq. (4)]. This interface defect is amphoteric and introduces two interface states within the band gap. Between room temperature and at least 125 °C, interface states are formed,¹¹ as shown in Eq. (4). In contrast, above about 230 °C, the H_2 and P_b centers react and form Si-H bonds.³⁰

The reaction sequence predicts a decrease of N_{ot} that is independent of gate bias and an increase of N_{it} only under positive bias. Both changes are in good agreement with the experimental results. The N_{ot} decrease shown in Fig. 5 is mainly due to H_2 and exhibits a weak polarity dependence. This weak dependence is due to the small, polarity-dependent contribution³¹ to the N_{ot} decrease that occurs without introducing H_2 .²⁵ Figure 4 shows that N_{it} increases much more with positive polarity than with negative polarity. There is a small increase of interface states due to H_2 under negative bias which may be explained within the framework of our model as follows. In Eq. (2) the cracking of H_2 and H^+ formation is shown as a single step. However, as discussed in Sec. V, Eq. (2) can be considered a two-step process in which free atomic hydrogen H^0 is formed as an intermediate step. Part of the H^0 may escape to create P_b centers. Because H^0 is neutral, its contribution to N_{it} formation is polarity independent. Note that H^0 can be substituted for $H^+ + e^-$ in Eq. (4) and the same interface defect is formed.²⁰ As discussed in Sec. V, H^0 is very reactive and most of it is expected to form H^+ . This interpretation is supported by cryogenic irradiation experiments in which there is evidence that H^+ formation is a two-step process; H^0 is created by the irradiation and most of it reacts with self-trapped holes to form H^+ .^{20,32}

This reaction sequence also predicts that each cracking site produces one H^+ hydrogen ion. Once the cracking site reacts, it is no longer chemically active. If the bias is initially negative, the H^+ produced during the negative bias interval drifts to the gate and does not produce interface states. A subsequent change to positive bias will not form many interface states because many of the cracking sites have already reacted. This is shown by the open diamond in Fig. 4; after 95 h in hydrogen under negative bias the bias is switched to positive for 80 h. The subsequent N_{it} increase is negligible compared to the increase under positive bias immediately after introducing H_2 . During the initial negative bias for 95 h, the H^+ produced drifts to the gate and its effect at the gate is not electrically observable. During the following 80 h under positive bias, only a small amount of H^+ is produced because most of the cracking sites have already reacted.

The nearly two-to-one ratio between ΔN_{it} and $-\Delta N_{ot}$ indicates that most of the H^+ created by cracking reaches the Si/SiO₂ interface. For each neutralized cracking site, one H^+ reaches the interface and creates one amphoteric defect such as a P_b center (introducing two states in the band gap). Similar results have been observed following pulsed irradiation.³³ These experiments estimate that 1.4 states are created for each H^+ . Given the experimental errors of both studies and the modeling uncertainties of Ref. 33, we consider the results to be in good agreement.

For the reaction sequence, Eqs. (1)–(4), the time dependence of N_{ot} and N_{it} shown in Figs. 1 and 3–5 indicate that Eq. (2) is the rate limiting step over most of the time range of the figures. The changes after introducing H_2 occur at a slower rate than interface reactions or diffusion of H_2 or H^+ . Pulsed irradiation results^{7,8} indicate that H^+ motion [Eq. (3)] and interface defect formation [Eq. (4)] are not the rate limiting steps. Within an hour after the irradiation pulse at least 80% of the interface-state buildup has occurred. This time scale is much shorter than the time scale observed in our experiments. The diffusion of H_2 into the gate oxide is not a rate limiting step except at the earliest times. Using H_2 diffusion constants obtained from bulk α -SiO₂ studies, the time for the hydrogen to diffuse into the gate oxide from the channel edges and reach half of its equilibrium concentration in a 5 or 10- μ m-long MOSFET is ~ 0.2 or ~ 0.7 h, respectively.^{21,22} The time scale of the N_{ot} and N_{it} changes in Figs. 1 and 3–5 are longer by at least two orders of magnitude. The rapid cessation of N_{it} and N_{ot} changes following the removal of the H_2 ambient in Figs. 1 and 3 is consistent with bulk α -SiO₂ H_2 diffusion constants. When the 5- μ m-long MOSFET is removed from the H_2 ambient, the H_2 diffuses out of the gate oxide, and the hydrogen concentration falls exponentially at a rate of one decade per hour.

We can apply a simple first-order kinetic theory to calculate the time dependence of the H_2 cracking which is the rate limiting step for the experimentally observed N_{ot} and N_{it} changes over most of the time shown in Figs. 1 and 3–5. We appeal to Brower's work on passivation of P_b centers for the model,³⁰ stated mathematically in Eq. (5), because our physical situation is similar,

$$[N_{or}] = N_0 \exp(-k_f[H_2]t). \quad (5)$$

Here, $[N_{or}]$ is the volume concentration of cracking sites at time t , N_0 is the initial value, k_f is the forward reaction rate constant, and $[H_2]$ is the volume concentration of hydrogen molecules as given by Shelby.²¹ The temperature dependence of k_f is given by³⁰

$$k_f = k_{of} \exp(-E_A/kT). \quad (6)$$

We use the same prefactor as Brower, $k_{of} = 1.9 \times 10^{-6}$ cm³/s, a saturation value of $N_0 = 3 \times 10^{11}$ /cm², and treat E_A as a parameter adjusted to fit the data in Fig. 3 to Eq. (5). We obtained two values for E_A , one for the first 4 h and one for the 28 h period between times b and c in Fig. 3. The first interval gives $E_A = 0.9$ eV and the later interval gives $E_A = 0.95$ eV. We interpret the different E_A values as a spread of activation energies over this range.

V. CRACKING SITE CALCULATIONS

The model set out in Sec. IV depends on the activation energy for cracking H_2 and forming mobile H^+ being roughly 1.0 eV or less. We appeal to semiempirical molecular orbital theory for estimates of the activation energy, as well as the energy of reaction for likely cracking sites. It is clear that a defect is required for efficient cracking because prior to irradiation there are no D_{it} or N_{ot} changes in MOSFETs placed into a H_2 ambient. Also, H_2 diffuses over long distances in bulk α -SiO₂ without being cracked. Two different types of hydrogen cracking sites have been tested by a series of molecular orbital calculations: oxygen vacancies (E' centers), and a broken Si—O bond hole trap (BBHT). E' centers are created in large numbers during irradiation.³⁴ Of the positively charged defects identified after irradiation, it has been studied most carefully. Furthermore, Lenahan and Dressendorfer have shown that at room temperature there is a strong correlation between the number of radiation induced E' centers measured by ESR and the total radiation-induced positive charge in MOS capacitors.³⁴ On the other hand, Brower, Lenahan, and Dressendorfer¹² have observed ESR spectra of oxygen-related centers, rather than E' centers, in MOS oxides γ irradiated at 4 K. Griscom^{35,36} has identified these low-temperature defects as self-trapped holes (STH) in the nonbonding $2p$ states of bridging oxygen ions in the glass network. In electrical measurements on MOS devices, Harari, Wang, and Royce³⁷ have observed trapped positive charge that has a similar low-temperature annealing behavior. We have extended this picture of self-trapping to the case in which the bonds are so severely strained that a Si—O bond is ruptured when a hole is trapped. In the reaction of H_2 with either E' or BBHT defects, one of the hydrogen atoms is tightly bound to Si or O, and the other forms a small polaron (H^+). The polaron consists of a positively charged, bridging oxygen attached to two silicon atoms and a hydrogen atom. Once formed, the H^+ polaron moves through the oxide by hopping among the bridging oxygen atoms.

We have applied MOPN,³⁸ a semiempirical molecular orbital program based on the modified intermediate neglect

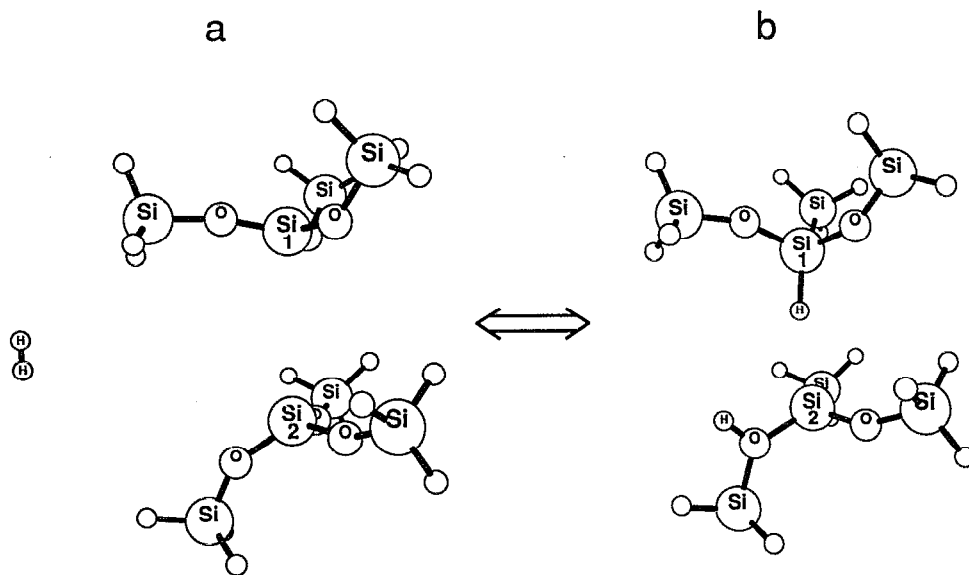


FIG. 6. Cluster used for the molecular orbital calculation of the reaction of the E' center with H_2 . In (a) the H_2 molecule and E' center are separated and the positive charge is localized primarily at Si_2 of the E' center. In (b), the two hydrogen atoms bond to Si_1 and the threefold coordinated oxygen atom. The positive charge is primarily localized on the same oxygen atom.

of differential overlap (MINDO/3),³⁹ to the atomic clusters shown in Figs. 6 and 7 to study the relative stability of the reactants and products in Eq. (2) for the two types of cracking sites. We have also calculated an approximate activation energy for each type of site. The calculations are important because, as shown below, they predict that one of these two defects is the more likely cracking site. The particular version of MOPN used has been modified to include a Saunders–Hillier⁴⁰ scheme to aid convergence.⁴¹ The clusters for each model were constructed by the same procedure. The initial strain on the central Si-O-Si or Si-Si unit was chosen by fixing $R_{Si_2-Si_1}$. The rest of the cluster was then built away from the core requiring that $R_{Si-O} = 1.63 \text{ \AA}$, the Si-O-Si angle = 144.0° , and the O-Si-O angle = 109.5° . We chose a distribution of dihedral angles to simulate an amorphous solid. This construction was used to fix the outer cage of atoms (the SiH_3 units in Fig. 6 and the OH units in Fig. 7). The strain is varied by changing the initial $R_{Si_2-Si_1}$ distance which sets the positions of the terminating atoms.

A. E' center

The first oxide hole trap that is considered for cracking H_2 and forming the H^+ small polaron is the E' center (oxygen vacancy). Based on previous experience with the peroxy radical,⁴² we considered two different sizes for the vacancy. We choose $R_{Si_2-Si_1} = 3.2 \text{ \AA}$, slightly larger than the α -quartz value, and $R_{Si_2-Si_1} = 4.2 \text{ \AA}$, the size for which the experiment and theory agreed for E' transformation into a peroxy radical. In the cracking calculations, the six outer silicon atoms and the 18 terminating hydrogen atoms are fixed, while the six oxygen atoms, the two inner silicon atoms (Si_1 and Si_2 in Fig. 6), and the two hydrogen atoms

that originally comprised the H_2 molecule move freely in search of a minimum energy configuration.

Figure 6 shows the products and reactants. After reacting, one of the hydrogen atoms passivates the original dangling silicon orbital (Si_1). The positive charge originally associated with the opposing Si atom (Si_2) moves to a neighboring oxygen atom and the second hydrogen atom bonds to that oxygen atom forming a threefold coordinated oxygen. The subsequent motion of H^+ is accomplished by hopping of the hydrogen atom and positive charge to other bridging oxygen ions.

The energies of the products and reactants are shown in Table I. Note that the relative stability of the products and reactants depends strongly on the size of the vacancy. Both reactions are endothermic; the energy is raised 1.2 eV for the less strained cluster and 0.5 eV for the more strained cluster. While for both sizes the reactants are more stable than the products, the energy difference is small enough to allow for significant concentrations of both reactants and products at room temperature.

The calculations for the activation energies are started with the final equilibrium geometry with one hydrogen atom passivating the dangling silicon orbital (Si_1) and one attached to a threefold coordinated oxygen atom. The H-H distance is the reaction coordinate. For both vacancy sizes, the activation energy is larger than 1.7 eV and in each case the potential barrier is a simple single hump. In similar calculations involving the passivation of the P_b center,⁴³ our calculations underestimated the measured activation energy by 18%. Because these systems are similar, the experimental activation energy is not expected to be lower than 1.7 eV. Thus, it is unlikely that the E' center cracks H_2 at room temperature.

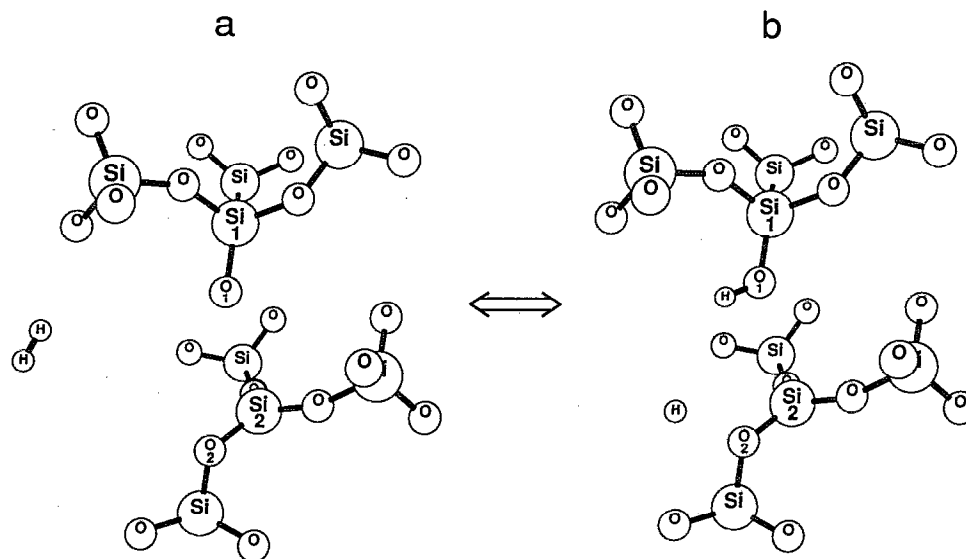


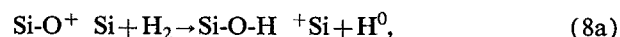
FIG. 7. Cluster used for the molecular orbital calculation of the reaction of a broken bond hole trap with H_2 . The hydrogen atoms in the terminating OH groups are omitted. In (a), the positive charge is primarily localized on O_1 . In (b), the intermediate products [rhs of Eq. (8a)] are shown. One hydrogen atom is bonded to O_1 and there is a free hydrogen atom. It reacts with one of the oxygen ions bonded to Si_2 [Eq. (8b)] to form a threefold coordinated, positively charged oxygen atom.

B. Broken Si—O bond

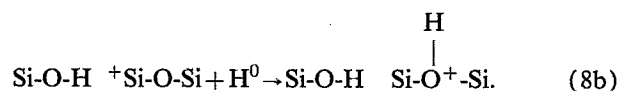
The second oxide hole trap that is considered for cracking H_2 and forming the H^+ small polaron is a broken Si—O bond. Unlike the E' center, there is not previous theoretical work showing that the defect is a stable hole trap. Because this is the first calculation to find localization of a hole in a SiO_2 network without oxygen vacancies, it is worthwhile to describe the model in detail. We envision a highly strained segment of the α - SiO_2 network such as exists near the Si/ SiO_2 interface.⁴⁴ If one of the Si—O bonds is extended sufficiently beyond the normal equilibrium length (~ 1.61 Å), to make the associated bonding level either degenerate with, or above, the SiO_2 valence-band edge, holes would preferentially trap there.



If the strained Si—O bond is a stable hole trap, it may crack a H_2 molecule in Eq. (2). The cracking is broken into two stages. In the first of the cracking stages a free hydrogen atom is produced. Specifically,



In the second stage the isolated H atom traps on one of the oxygen atoms backbonded to the ^+Si on the rhs of Eq. (8a), taking the positive charge with it:



In Eq. (8b), we include one of the three oxygen atoms backbonded to the silicon atom on the right side of the defect to illustrate the charge transfer from the silicon atom to the threefold coordinated oxygen moiety. The threefold coordinated oxygen ion can be thought of as a small polaron dressed with a hydrogen atom. This polaron is assumed to be mobile enough to diffuse under positive bias through the lattice. Certainly the experimental data of McLean supports this assumption.⁷ The calculations performed here address hole trapping [Eq. (7)] and H_2 cracking [Eqs. (8a) and (8b)]. By calculating equilibrium geometries and charge densities, we establish predicted precursors that lead to bond scission and hole trapping. By calculating total energies of reactants and products, as well as a reaction path, we can estimate the activation energy for cracking and the stability of the products against recombination into H_2 . As discussed above, the calculated activation energy supports the conclusion that H_2 cracking is the rate limiting step to changes in N_{it} and N_{ot} [Eqs. (1)–(4)] over most of the time range examined.

We tried a variety of cluster geometries and termination schemes to localize a hole on one oxygen atom sur-

TABLE I. Total energies for the end points of the reaction of H_2 with E' centers as a function of vacancy size. Energies are in eV.

Cluster configuration	E_{tot} ($R_{in}=3.2$ Å)	E_{tot} ($R_{in}=4.2$ Å)
$H_2 + Si^+ Si$	−2944.19	−2944.49
$Si-H \quad \begin{array}{c} H \\ \\ Si-O^+-Si \end{array}$	−2943.03	−2943.96
ΔE	1.17	0.53

TABLE II. Bond strain on the three shells of oxygen atoms of the cluster shown in Fig. 7 in the neutral and positive charge states as measured by the deviation from the MINDO/3 equilibrium Si—O bond length, 1.63 Å.

Shell	Strain ⁰ (Å)	Strain ⁺ (Å)
18 outer oxygen atoms	−0.14–0.04	−0.036–0.01
6 intermediate oxygen atoms	0.04–0.08	−0.060–0.07
Central oxygen atom	0.106–0.14	0.08–1.19

rounded by two silicon atoms. Allowing the seven oxygen atoms and eight silicon atoms to move freely to minimize total energy, we found that we had to use the following constraints.

(i) The terminating SiH₃ units were replaced with Si(OH)₃ units. Without this replacement, the hole never traps on the central oxygen atom. If the terminating hydrogen atoms are part of SiH₃ groups, the molecular orbitals with significant SiH character interact strongly with the oxygen lone-pair orbitals that form the highest occupied molecular orbital (HOMO). This interaction drove the HOMO level 1.24 eV above the nearest occupied molecular orbital with substantial lone-pair character on the central oxygen atom. Thus, during a typical self-consistent field calculation a hole would never be localized on this atom. With terminating OH groups, the HOMO was only ~0.5 eV above the nearest central oxygen lone-pair state.

(ii) The initial Si₂–Si₁ separation was 4.5 Å, so that the initial Si₁–O₁ and Si₂–O₁ distances were large enough to guarantee bond scission in the positive charge state if the calculation was not started at the neutral equilibrium.

If we minimize the energy in the neutral charge state (with the initial $R_{\text{Si}_2\text{--Si}_1} = 4.5$ Å), the strain that was initially restricted to the three central atoms is distributed over the whole cluster, as seen in the middle column of Table II. (In this calculation, the equilibrium value for $R_{\text{Si}_2\text{--Si}_1}$ is 3.48 Å.) If the positive charge state calculation is started in this geometry, 50% of the positive charge and 91% of the spin are localized on one of the outer oxygen atoms. To achieve this localization, one of the outer Si—O bond lengths increases to 1.85 Å. The central oxygen atom is bonded to the two central silicon atoms, but the bonding is more asymmetric than in the neutral case ($R_{\text{Si--O}} = 1.69$ and 1.80 Å). On the other hand, if we start the positive charge state calculation with all the strain restricted to the three central atoms, we find that the equilibrium geometry of the central atoms is much more asymmetric. The Si—O bond lengths for the central oxygen atom are 1.72 and 2.82 Å, indicating that the latter bond is nearly broken. The percentage of positive charge is localized on the central oxygen atom is 28% (O₁ in Fig. 7), 10% on the opposing Si atom (Si₂), and the rest of the charge is distributed among the remaining atoms. Most of the spin density (96%) is localized in the lone-pair 2p orbital of the O₁.

The existence of two equilibrium geometries implies that one of them is metastable. The total energy of the more asymmetric cluster is 0.5 eV lower. Thus, we conclude that the localization of the hole on one of the outer OH groups is an artifact of the finite cluster size, and that

TABLE III. Total energies for the critical points of reaction of Eq. (8).

Cluster configuration	E_{tot} (eV)
H ₂ + Si-O ⁺ Si	−8902.54
H ₂ + Si-O-H + Si	−8902.82
Transition state	−8901.61
$\begin{array}{c} \text{H} \\ \\ \text{Si-O-H} \quad \text{Si-O}^+\text{-Si} \end{array}$	
ΔE	−1.49

charge trapping on the central oxygen atom is to be expected.

We now turn to the second stage of the BBHT model, the cracking of H₂. In these calculations, we hold $R_{\text{O}_1\text{--H}}$ fixed (as well as all the geometric parameters associated with the terminating OH groups) while allowing all other geometrical parameters to vary. The equilibrium geometries for the lhs and rhs of Eq. (8a) are shown in Fig. 7. We should point out that when the central O—H bond forms [Fig. 7(b)], the positive charge hops onto the threefold coordinated silicon atom (Si₂), which relaxes into the plane of its three nearest neighbors. In Table III, we give the energies of the critical points of the reaction shown in Eq. (8). Note that the cracking reaction at this defect is exothermic by 0.29 eV. This is not surprising; the O—H bond is very stable, and in both the initial and final states, there is one unsatisfied bond.

In the final stage of cracking, the free hydrogen atom, H⁰ in the rhs of Eq. (8a), reacts to form a threefold coordinated oxygen atom (such as O₂ in Fig. 7). There is no barrier to Eq. (8b) and in the equilibrium geometry of the rhs of the reaction, the total energy is lowered an additional 1.2 eV. Thus, we expect that most of the H⁰ created in Eq. (8a) will be transformed to H⁺ by Eq. (8b). As discussed earlier, the larger N_{it} buildup under positive polarity indicates that most of the H⁰ is converted to H⁺ before diffusing to the Si/SiO₂ interface and forming P_b defects. It is also reasonable that a small fraction of the H⁰ may escape and form P_b defects. This would explain the small number of interface states formed under negative polarity.

While it is encouraging that the simple H₂ cracking is predicted to be exothermic, the more conclusive result is the activation energy for this process. The activation energy for simultaneous H₂ dissociation and O—H bond formation has been calculated in the forward and reverse directions. Consider the reverse reaction. Starting with the equilibrium geometry shown in Fig. 7(b), the isolated hydrogen is moved toward the central OH group using $R_{\text{H--H}}$ as the reaction coordinate. All atoms except the outer cage of OH groups were allowed to relax. We found that the central O—H bond does not break spontaneously to allow formation of a H₂ molecule. Rather, when $R_{\text{H--H}} \sim 1.0$ Å, it was necessary to switch the reaction coordinate to $R_{\text{H--O}_1}$ and again allowing all atoms except the OH cage to relax. Thus, the reverse reaction (formation of H₂) proceeds as

follows. An isolated hydrogen atom approaches the OH group. As it comes within roughly 1.0 Å of the bonded hydrogen atom, the O—H bond must simultaneously stretch for the H—H bond to form. The shape of the barrier is a simple single hump and the activation energy is 1.1 eV. We have also calculated the activation barrier for the forward reaction starting with an isolated H₂ and ending with an OH group and an isolated H atom. The resulting activation energy is within a few hundredths of an eV of our first estimate.

These calculations demonstrate that BBHTs, which are similar to nonbridging oxygen hole centers (NBOHCs), are efficient cracking sites for H₂. The calculated activation energy for the BBHT is in good agreement with the estimates based on fitting first-order kinetics to the experimental data in Fig. 3.

In closing this section we should point out that the geometry used here is probably not the only one that leads to strained bond hole trapping and H₂ cracking. With less strain than used in the above calculations, we expect that it would be possible to have hole trapping without breaking Si—O bonds. We also expect that the strained bond hole trap would crack H₂. However, the current cluster technique introduces artifacts that preclude even qualitative confirmation. This will be discussed at length in a future publication.

VI. DISCUSSION AND CONCLUSIONS

The combined experiments and calculations presented in this paper support the model of hydrogen cracking at a broken Si—O bond and subsequent interface defect formation. The model accounts for the involvement of hydrogen, for the polarity dependence of the formation of interface defects, and for the polarity independence of the neutralization of trapped oxide positive charge. The model also explains why the reactions do not occur without first irradiating the gate oxide. The rate limiting step, the H₂ cracking, accounts for the time dependence of charge neutralization and interface-state formation. Furthermore, there is good agreement between the observed and the calculated activation energies for Eq. (8). However, we would be remiss if we did not underline some of the questions left unanswered by this study. First, all of the direct experimental evidence for self-trapped holes (STHs) has been obtained at low temperature in bulk α -SiO₂, and shows that the STHs are annealed well below room temperature. In contrast, the experiments described here were performed at room temperature. We are assuming that a defect similar to a STH is stabilized at room temperature by introducing greater strain, a reasonable but unverified assumption. It is supported by recent measurements in compressed bulk α -SiO₂ in which STHs are observed up to nearly room temperature.⁴⁵ We should also point out that near the Si/SiO₂ interface one would expect compressive strain in thermal SiO₂, while we have used tensile strain. We have been unable to study compressive strain because of difficulties with obtaining self-consistent-field convergence. However, for either compressive or tensile strain, the Si—O bonding levels are raised and we expect similar effects. Further-

more, we have suggested that a hole trapped at a bridging oxygen atom with highly strained bonds may also be a candidate for H₂ cracking. The calculations do not verify the model, but they do show that it is reasonable. They also predict an ESR signature of the cracking site. This ESR signal should look very much like a NBOHC, and it should decrease as N_{or} decreases.

Another interesting feature of the model is the 2:1 ratio of interface states generated to positive charges lost. We interpret this as the formation of a P_b defect with two levels in the band gap. In this model, each H⁺ resulting from positive charge annihilation reaches the Si/SiO₂ interface, captures an electron from the silicon substrate to become H⁰, and each H⁰ reacts with a passivated dangling orbital (Si—H) at the interface to form a P_b defect. It is possible that the 2:1 ratio is a result of the positive charge annihilation and interface state formation occurring at the same defect. That is, H₂ triggers the charge neutralization at the precursor of the interface defect. This possibility is similar to the hole-to-interface-state models that have been proposed.^{46,47} We believe this is unlikely to apply here for two reasons. First, it would require that a defect complex absorb two hydrogen atoms and leave a dangling orbital. Second, and possibly more important, if the positive charge trap were an interface defect precursor, it would be at the interface. This would remove the bias dependence of interface state formation.

Note that our model requires that a H⁰ reacts to form the interface defect before being consumed by any other reaction. This demands a sufficiently plentiful number of passivated dangling orbitals. Stesmans and Van Gorp⁴⁸ have obtained an interface density of $1.4 \times 10^{13}/\text{cm}^2$ passivated orbitals corresponding to an average separation of under 30 Å. We expect that this density is high enough for most of the H⁰ to encounter a passivated dangling orbital first.

The repeated introduction and removal of hydrogen and the associated changes in N_{it} and N_{or} demonstrate clearly the role hydrogen can play in the post-irradiation buildup of interface states. We believe that this experiment also addresses results obtained in the absence of a hydrogen ambient. There are strong similarities between interface state formation by irradiation and by cracked H₂. Both processes yield the same energy distribution of interface states. Even more striking are comparisons of our results with pulsed irradiation experiments.^{33,49} Following the radiation pulse, the buildup of interface states is monitored for times ranging from milliseconds to thousands of seconds. The interface formation consists of a small “prompt” component that occurs before the first measurements and a larger interface-state buildup that saturates within thousands of seconds. As in our experiments, the latter contribution to interface states has been attributed to H⁺ transport through the oxide, and the buildup only occurs under positive bias. Furthermore, if the bias is switched to negative at any time, the buildup stops⁴⁹ because H⁺ no longer drifts to the interface. Another pulsed irradiation experiment used midgap voltage changes to monitor the motion of H⁺ through the gate oxide and

correlated the motion to interface state buildup.³³ The best fit to the data of this experiment yields 1.4 interface states formed for each H^+ generated. Our results which show there is a two-to-one ratio between interface states formed and trapped charges neutralized. Assuming each neutralized charge creates one H^+ and that most interface states are formed by H^+ , our results show two interface states formed by each H^+ . Thus, the results of both types of experiments indicate that each interface defect introduces two interface states (e.g., an amphoteric defect such as a P_b center).

To conclude, we have presented a combined experimental and theoretical study of a model for the post-irradiation buildup of interface states and the simultaneous depletion of oxide fixed positive charge. This model involves the cracking of H_2 at radiation-induced, positively charged defects, and the subsequent transport of H^+ to the Si/SiO₂ interface where it captures an electron from the silicon substrate and then reacts with an interfacial Si-H to form a dangling-bond defect and H_2 . The experimental data show clearly that the increase of N_{it} and the decrease in N_{of} are correlated with the presence of H_2 . Allowing for a distribution of activation energies, the H_2 cracking reaction is consistent with first-order kinetics with activation energies in the range of 0.90–0.95 eV. We have performed calculations on two types of positively charged defects that could crack H_2 , oxygen vacancies (E' centers) and broken bond hole traps (BBHTs). We find that the latter is the more likely candidate for cracking H_2 because (i) the cracking reaction is exothermic for the BBTH and endothermic for the E' center, and (ii) the calculated activation energy of H_2 cracking is 1.1 eV for the BBTH and greater than 1.7 eV for the E' center. Finally, based on the similar effects observed in this study and in radiation studies, we believe that the role of hydrogen in forming interface states by irradiation is confirmed.

ACKNOWLEDGMENTS

The authors wish to thank M. E. Zvanut for discussions about the article. We also gratefully acknowledge the Office of Naval Research for its support and North Carolina Supercomputer Center for a generous grant of supercomputer time. We wish to thank K. Flurchick for his assistance in optimizing MOPN on the CRAY Y-MP.

- ¹E. H. Nicollian, C. N. Berglund, P. F. Schmidt, and J. M. Andrews, *J. Appl. Phys.* **42**, 5654 (1971).
- ²E. H. Nicollian, A. Goetzberger, and A. D. Lopez, *Solid-State Electron.* **12**, 937 (1969).
- ³D. J. DiMaria and J. W. Stasiak, *J. Appl. Phys.* **65**, 2342 (1989).
- ⁴K. G. Aubuchon, *IEEE Trans. Nucl. Sci.* **NS-18**, 117 (1971).
- ⁵Y. Nissan-Cohen, *Appl. Surf. Sci.* **39**, 511 (1989).
- ⁶P. S. Winokur, in *Ionizing Radiation Effects in MOS Devices and Circuits*, edited by T. P. Ma and P. V. Dressendorfer (Wiley, New York, 1989).
- ⁷F. B. McLean, *IEEE Trans. Nucl. Sci.* **NS-27**, 1651 (1980).

- ⁸N. S. Saks and D. B. Brown, *IEEE Trans. Nucl. Sci.* **NS-36**, 1848 (1989).
- ⁹L. Do Thanh and P. Balk, *J. Electrochem. Soc.* **135**, 1797 (1988).
- ¹⁰R. A. Kohler, R. A. Kushner, and K. H. Lee, *IEEE Trans. Nucl. Sci.* **NS-35**, 1492 (1988).
- ¹¹R. E. Stahlbush, B. J. Mrstik, and R. K. Lawrence, *IEEE Trans. Nucl. Sci.* **NS-37**, 1641 (1990).
- ¹²K. L. Brower, P. M. Lenahan, and P. V. Dressendorfer, *Appl. Phys. Lett.* **41**, 251 (1982).
- ¹³D. L. Griscom, M. Stapelbroek, and E. J. Friebele, *J. Chem. Phys.* **78**, 1638 (1983).
- ¹⁴D. L. Griscom, *J. Non-Cryst. Solids* **68**, 301 (1984).
- ¹⁵R. Gale, F. J. Feigl, C. W. Magee, and D. R. Young, *J. Appl. Phys.* **54**, 6938 (1983).
- ¹⁶J. E. Shelby, *J. Appl. Phys.* **50**, 3702 (1979).
- ¹⁷J. E. Shelby, *J. Appl. Phys.* **51**, 2589 (1980).
- ¹⁸R. A. Weeks, *Phys. Rev.* **130**, 570 (1963).
- ¹⁹F. J. Feigl, W. B. Fowler, and K. L. Yip, *Solid State Commun.* **14**, 225 (1974).
- ²⁰D. L. Griscom, D. B. Brown, and N. S. Saks, in *The Physics and Chemistry of SiO₂ and the Si-SiO₂ Interface*, edited by C. R. Helms and B. E. Deal (Plenum, New York, 1988), p. 287.
- ²¹J. E. Shelby, *J. Appl. Phys.* **48**, 3387 (1977).
- ²²J. Crank, *The Mathematics of Diffusion* (Clarendon, Oxford, 1975), p. 50.
- ²³G. Groeseneken, H. E. Maes, N. Beltran, and R. F. deKeersmaecker, *IEEE Trans. Electron. Devices* **ED-31**, 42 (1984).
- ²⁴N. S. Saks and M. G. Ancona, *IEEE Trans. Nucl. Sci.* **NS-34**, 1348 (1987).
- ²⁵T. R. Oldham, A. J. Lelis, and F. B. McLean, *IEEE Trans. Nucl. Sci.* **NS-33**, 1203 (1986).
- ²⁶P. S. Winokur, H. E. Boesch, Jr., J. M. McGarrity, and F. B. McLean, *J. Appl. Phys.* **50**, 3492 (1979).
- ²⁷T. P. Ma, *Semicond. Sci. Technol.* **4**, 1061 (1989).
- ²⁸R. E. Stahlbush, R. K. Lawrence, and W. Richards, *IEEE Trans. Nucl. Sci.* **NS-36**, 1998 (1989).
- ²⁹G. J. Gerardi, E. H. Poindexter, and P. J. Caplan, *Appl. Phys. Lett.* **49**, 348 (1986).
- ³⁰K. L. Brower, *Appl. Phys. Lett.* **53**, 508 (1988).
- ³¹A. J. Lelis, T. R. Oldham, H. E. Boesch, Jr., and F. B. McLean, *IEEE Trans. Nucl. Sci.* **NS-35**, 1186 (1988).
- ³²N. S. Saks, R. B. Klein, and D. L. Griscom, *IEEE Trans. Nucl. Sci.* **NS-35**, 1234 (1988).
- ³³N. S. Saks and D. B. Brown, *IEEE Trans. Nucl. Sci.* **NS-37**, 1624 (1990).
- ³⁴P. M. Lenahan and P. V. Dressendorfer, *J. Appl. Phys.* **55**, 3495 (1984).
- ³⁵D. L. Griscom, *Phys. Rev. B* **40**, 4224 (1989).
- ³⁶D. L. Griscom, *J. Non-Cryst. Solids* **149**, 137 (1992).
- ³⁷E. Harari, S. Wang, and B. S. H. Royce, *J. Appl. Phys.* **46**, 1310 (1975).
- ³⁸P. Bischof, *J. Am. Chem. Soc.* **98**, 6844 (1976).
- ³⁹R. C. Bingham, M. J. S. Dewar, and D. H. Lo, *J. Am. Chem. Soc.* **97**, 1285 (1975).
- ⁴⁰V. R. Saunders and I. H. Hillier, *Int. J. Quantum Chem.* **7**, 699 (1973).
- ⁴¹We gratefully acknowledge P. Deak for allowing us to use this version of MOPN.
- ⁴²A. H. Edwards and W. B. Fowler, *Phys. Rev. B* **26**, 6649 (1942).
- ⁴³A. H. Edwards, *Phys. Rev. B* **36**, 9638 (1987).
- ⁴⁴F. J. Grunthaner, P. J. Grunthaner, and J. Maserjian, *IEEE Trans. Nucl. Sci.* **NS-29**, 1462 (1982).
- ⁴⁵D. L. Griscom (unpublished).
- ⁴⁶S. K. Lai, *Appl. Phys. Lett.* **39**, 58 (1981).
- ⁴⁷G. Hu and W. C. Johnson, *J. Appl. Phys.* **54**, 1441 (1983).
- ⁴⁸A. Stesmans and G. Van Gorp, *Phys. Rev. B* **42**, 3765 (1990).
- ⁴⁹J. M. McGarrity, P. S. Winokur, H. E. Boesch, Jr., and F. B. McLean, in *Physics of SiO₂ and Its Interfaces*, edited by S. T. Pantelides (Pergamon, New York, 1978).